Composites Part B 158 (2019) 319–327

Contents lists available at ScienceDirect

Composites Part B

journal homepage: www.elsevier.com/locate/compositesb

Topological optimization of thermoelastic composites with maximized stiffness and heat transfer

A.V. Krysko[a,b], J. Awrejcewicz[c,*], S.P. Pavlov[d], K.S. Bodyagina[d], V.A. Krysko[d]

[a] Department of Applied Mathematics and Systems Analysis, Saratov State Technical University, 410054, Saratov, Politehnicheskaya 77, Russian Federation
[b] Cybernetic Institute, National Research Tomsk Polytechnic University, 634050, Tomsk, Lenin Avenue, 30, Russian Federation
[c] Lodz University of Technology, Department of Automation, Biomechanics and Mechatronics, 1/15 Stefanowskiego St, 90-924, Łódź, Poland
[d] Saratov State Technical University, Department of Mathematics and Modelling, Politehnicheskaya, 77, Saratov, 410054, Russian Federation

ARTICLE INFO

Keywords:
Metal-matrix composites (MMCs)
Mechanical properties
Thermal properties
Computational modelling

ABSTRACT

The topological optimization of composite structures is widely used while tailoring materials to achieve the required engineering physical properties. In this paper, the problem of topological optimization of the microstructure of a composite aimed at the construction of a material with most effective values of the bulk modulus of elasticity and thermal conductivity taking into account competing mechanical and thermal properties of the materials included in the composite is defined and solved. A two-phase composite consists of two base materials, one of which has a higher Young modulus but lower thermal conductivity, while the other has a lower Young modulus but higher thermal conductivity. A new class of problems for composites containing material pores or technological inclusions of different shapes is considered. Effective thermoelastic properties are obtained using the asymptotic homogenization method. A modified solid isotropic material with penalization (SIMP) model is used to regularize the problem. The problem of the isoperimetric constraints is solved by the method of moving asymptotes (MMA). The influence on optimal topology of the composite in the presence of two competing materials, and optimality criteria using linear weight functions are investigated. Pareto spaces that provide deep understanding of how these goals compete in achieving optimal topology are constructed.

1. Introduction

The use of new composite materials requires a theoretical background to predict microscopic/effective properties of composites based on the knowledge of their material components. It is well known and documented that cell bulk fractions, shapes, and orientation are important factors in the manufacturing of composite materials with the effective properties.

The topological optimization of composite structures is a widely employed method of tailoring materials, used to achieve their improved and required physical properties. In the recently published papers and monographs, one can find that the asymptotic homogenization approach plays a key role in achieving reliable averaging of the complex microstructural behaviour of an elastic medium [1–4]. An interesting way to compute modified Young modules in both directions for a two-dimensional crystal body with a square lattice using the continuum approach of continuum mechanics is described in Ref. [43].

It appears that the most widely recognized and used methods for the topological optimization of structures are explicit parametrization methods, which are known as density-based methods. These methods are based on the subdivision of the analyzed mechanical object into finite elements. Instead of a set of properties, each finite element contains only one design variable, which is often understood as the finite element material density ρ_e. The main idea of this approach is to define the finite element parameters as design variables and derive a relationship between local (for instance, density) and global physical properties of the material (for instance, Young modulus or thermal conductivity) in the computational process aimed at finding parameters in the optimization process. To design microstructures composed of different materials, the SIMP (Solid Isotropic Material with Penalization) method [5], the evolutionary structural optimization (ESO) [6], and the level set method (LS) [7–10] are used. In particular, the use of the homogenization with SIMP is becoming increasingly popular and useful.

By virtue of numerous algorithms aimed at finding an optimum, such as the method of optimal criterion (OC) [11], successive linear

* Corresponding author.
E-mail addresses: anton.krysko@gmail.com (A.V. Krysko), jan.awrejcewicz@p.lodz.pl (J. Awrejcewicz), pspsar@yandex.ru (S.P. Pavlov), bodksen@mail.ru (K.S. Bodyagina), tak@san.ru (V.A. Krysko).

https://doi.org/10.1016/j.compositesb.2018.09.047
Received 27 July 2018; Received in revised form 5 September 2018; Accepted 19 September 2018
Available online 22 September 2018
1359-8368/

programming (SLP) or the method of moving asymptotes (MMA) [12], the optimized material localization allows us to achieve the required functional material characteristics. The current research has focused on solving problems aimed at either optimizing the constructions [3,6,8] or getting functional properties of materials [13–19]. When designing composite structures, either elastic or thermal/thermoelastic properties are usually taken into account. In the case of the elasticity criterion, only the mechanical load is considered [3,39], whereas thermal criteria take into account the thermal load [20,21], and thermoelastic criteria cover both mechanical and thermal loads [22,23].

It should be emphasized that there are two approaches that include both thermal and mechanical criteria in topological optimization problems. The first one considers the material as thermoelastic without the coupling between the thermal and mechanical fields in the topological sense (the thermal load is converted into mechanical load) [22,23]. In this case, the structure is controlled by the mechanical characteristics. On the other hand, the second approach takes into account both the heat and mechanical fields. Namely, the temperature field is considered first, and then it is matched with the field of deformations. In the mentioned cases, the design can be guided either by the mechanical target function [23] or by coupled mechanical and heat functions [24].

The qualitative seminal results in the problem of design of materials were obtained by Sigmund [15,16] who introduced the method of inverse optimization. It is assumed that the composites are built from identical periodic base cells. The methodology of the topological optimization was employed in the case of the proper distribution of one-component [14] or multi-phase materials [18,19] in order to achieve the required physical properties. It is known that direct homogenization makes it possible to consider global properties based on a structure of the elementary cell or the representative volume [25]. On the other hand, the inverse homogenization is aimed at searching the optimized material distributions within the elementary cell [14]. Differences between the global homogenized material properties and their target values are minimized with the help of topological optimization methods [14,16,19]. In this context, the elastic and heat material properties are considered separately.

Optimal microstructures of materials have been developed in the problems of maximizing bulk and shear moduli [19,26]. Using this approach, novel composites with negative Poisson's coefficient [14] and materials with extreme or negative coefficients of thermal expansion [16] have been designed, which demonstrated wide possibilities of this method in the design of elastic and thermoelastic composites.

On the other hand, in many cases, the heat transfer and elastic properties of materials compete with each other [27]. Hence, it is often difficult to achieve both high heat transfer and high stiffness simultaneously. For this reason, it is important to develop a procedure that would work effectively in spite of the conflicting objectives. In general, the multi-target optimization is difficult or even impossible to obtain a global optimum for all expected design targets. However, in the optimization process, it can be seen that at some stage, any further improvement of one criterion requires a compromise with at least one other criterion. A set of such solutions determines the Pareto space which consists of a series of points within the solution space [28], where for each of the mentioned solutions it is impossible to further improve some target functions without worsening at least of one of the remaining target functions. Thus, it is necessary to gather as much information about the Pareto space as possible to choose the best solution.

Torquato et al. [29] combined heat transfer and electrical transfer with equal weight to propose the optimal design of manufacturable 3D composites with multifunctional characteristics. Yoo et al. [30] used various weight coefficients to find optimal topologies of the Pareto solution of a swing arm type actuator in accordance with the flexibility criteria and eigenfrequency. The mentioned works show that the use of the weight functions is the best method to obtain a set of Pareto solutions.

Seresta et al. [31] considered a wing box design optimization by employing composite laminates with blending constraints based on the inclusion of fibre orientation angle of the layers and the total thickness of the laminate as design optimization variables. They have shown that the optimum design has better continuity of the laminate lay-ups.

The multi-criteria (multi-objective) optimization of laminated composite structures under technological constraints was discussed by Bassir et al. [32]. The main method based on the NSGA-II program exhibited its efficiency in obtaining a uniform spray of the Pareto solutions.

Lee et al. [33] developed a multi-objective approach using a parallel multi-objective generic algorithm to study a stacking sequence design optimization for a multilayer composite plate. The used methodology matched a robust multi-objective evolutionary algorithm and a finite element analysis with a parallel optimization system. It has been shown analytically that Pareto optimal solutions offer a set of selections for engineers to improve the composite structure in terms of the industrial needs (cost) and mechanical properties (weight and stiffness).

Ning et al. [34] developed an experimental method of additive manufacturing using the fused deposition modelling, which affected the tensile strength, Young's modulus, yield strength, flexural stresses, and toughness of reinforced thermoelastic composites.

Madeira et al. [35] proposed the optimal design of laminated composite panels with constrained layer damping aimed at minimization of weight and maximization of model damping. In particular, trade-off Pareto optimal solutions and the respective treatment configurations were obtained and analyzed.

Salem and Donaldson [36] developed and studied a methodology for a combined weight and cost optimization of sandwich plates with hybrid composite face sheets and a foam core. The used multi-objective optimization technique allowed them to minimize both the weight and the cost of the hybrid sandwich plate simultaneously. The Pareto frontier trade of the curve was generated by optimizing a sequence of combining weight and cost objective functions.

Seretis et al. [37] carried out the multi-parameter design of experiments based on the multi-objective curing cycle optimization for glass fabric/epoxy composites by using the Poisson regression and generic algorithm. The authors achieved the estimation of the curing parameters for optimum tensile and flexural performance with high accuracy, and they demonstrated that the Poisson regression theoretical model can predict the tensile and flexural response of the cured composites accurately.

Passos and Luersen [38] employed the multi-objective optimization of curvilinear fibre composites in two cases: for a square plate and a fuselage-like section. The considered problems consisted of three to twelve variables in order to detect the resulting Pareto front properly. To overcome the long computational time needed by the finite element method, the Kriging-based approaches were used.

In this work we define and solve the problem of topological optimization of the composite microstructure in order to construct a material with the largest effective values of the Young modulus and thermal conductivity. The studied two-phase composite consists of two materials: the first one has high Young modulus and low thermal conductivity whereas the second one is characterized by low Young modulus and high thermal conductivity.

The work presents the study of the influence of two competing material properties, i.e. mechanical and thermal, using linear weight functions. In particular, the problem of construction of the Pareto spaces yielding an insight into the role of competing material properties in the optimal topologies is addressed. The paper can be treated as an extension of our earlier research [39].

The paper is organized in the following way. In Section 2 (3), the effective tensor of elastic properties (the effective heat transfer coefficient) of the studied composite with mechanical and heat parameters is defined. The topological optimization is carried out in Section 4. Numerical results of the topological optimization of a composite made: (i)

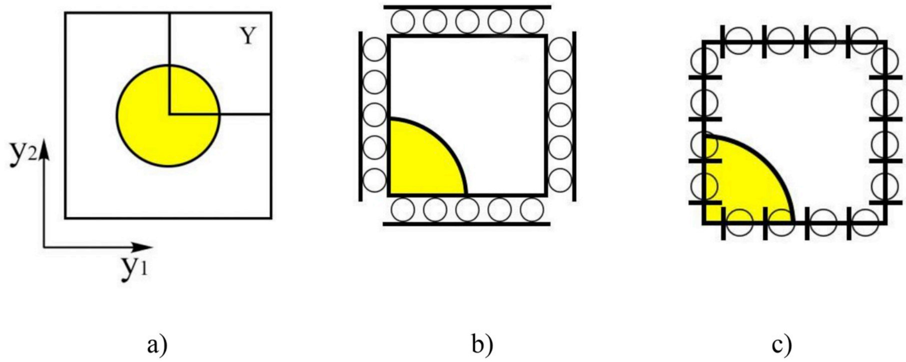

Fig. 1. Elementary periodic composite cell: (a) the area of topological optimization Y and boundary conditions for case (b,c) on the quarter of the base cell.

from two composite materials; (ii) with technological holes, and (iii) with technological inclusions are presented in Sections 5.1. 5.2 and 5.3, respectively. Concluding remarks (Section 6) sum up the study and the results obtained.

2. Determination of the effective tensor of elastic properties

In this work, the following assumptions are introduced: the composite is linearly elastic and macroscopically transversely isotropic with respect to both mechanical and heat parameters. Initial stresses are absent and the introduced inclusions are homogeneous, linearly elastic, isotropic, and regularly packed. The matrix is homogeneous, linearly elastic, and isotropic with respect to mechanical and thermal parameters. For composites consisting of linear elastic materials, the governing differential equations of a homogeneous and microstructural element are composed of linear elasticity equations.

In the elastic regime, the microscopic behaviour of the elementary periodic cell made from an anisotropic material can be described by the effective stress tensor $\bar{\sigma}_{ij}$ and deformation tensor $\bar{\varepsilon}_{ij}$ of a homogenized medium. The tensors are coupled by means of the effective elasticity tensor C^e_{ijkl}.

$$\bar{\sigma}_{ij} = C^e_{ijkl}\bar{\varepsilon}_{kl}, \tag{1}$$

and C^e_{ijkl} depends on the volume fraction of the filler and the microstructure of the elementary cell.

We introduce the local coordinate system (Y) to describe the rapid changes in properties of the microstructure of the material in the global coordinate system (X) in the macro scale. The local coordinate y can be considered as a fast coordinate which is coupled with x through the relation $y = x/\varepsilon$ $(\varepsilon << 1)$. The displacement of an arbitrary material point in an elastic body can be approximated using two-scale asymptotic series [40,41].

$$u^{\varepsilon}(x) = u^0(x,y) + \varepsilon\, u^1(x,y) + \varepsilon^2\, u^2(x,y) + \ldots \tag{2}$$

Substituting (2) into the equilibrium equations, the tensor of the effective elastic properties is obtained in the following form

$$C^e_{ijkl} = \frac{1}{|Y|}\int_Y \left(C_{ijkl} - C_{ijpq}\frac{\partial \chi_p^{kl}}{\partial y_q} \right) dY, \tag{3}$$

where $|Y|$ stands for the area of the elementary cell, χ_p^{kl} is a periodic field of the allowed displacements in the case of kl load [40] and it satisfies the following integral equations with respect to the elementary periodic cell with periodic boundary conditions

$$\int_Y C_{ijpq}\frac{\partial \chi_p^{kl}}{\partial y_q}\frac{\partial v_i}{\partial y_j} d\,Y = \int_Y C_{ijkl}\frac{\partial v_i}{\partial y_j} d\,Y, \qquad \forall\, \mathbf{v} \in Y. \tag{4}$$

Here $\mathbf{v}$ stands for the kinematically allowed arbitrary field of displacements.

Problem (4) is farther solved on the elementary cell by the FEM (finite element method). Along the boundaries of various phases, the coupling conditions are formulated. For the problem of a plane stress-strain state, there are two independent loading cases $kl = 11,\ 12$. Equation (3) can be recast to the following form

$$C^e_{ijkl} = \frac{1}{|Y|}\int_Y \left(C_{ijkl} - C_{ijpq}\frac{\partial \chi_p^{kl}}{\partial y_q} \right) dY = \langle C_{ijkl} \rangle - \langle \sigma_{ij}^{kl} \rangle, \tag{5}$$

where $\langle C_{ijkl} \rangle$ denotes the averaged elastic tensor dependent on the material volume fraction, which is estimated based on the classical mixture laws; $\langle \sigma_{ij}^{kl} \rangle$ denotes the averaged stress tensor on the elementary cell in the case of kl load. It is easy to notice that $\langle \sigma_{ij}^{kl} \rangle$ stands for a correcting term representing the influence of the material microstructure of the elementary cell. Formula (5) can be presented in the following form

$$C^e_{ijkl} = \frac{1}{|Y|}\int_Y C_{pqrs}(\varepsilon_{pq}^{0(ij)} - \varepsilon_{pq}^{*(ij)})(\varepsilon_{rs}^{0(kl)} - \varepsilon_{rs}^{*(kl)})\, d\,Y, \tag{6}$$

where $\varepsilon_{pq}^{*\,(ij)} = \frac{1}{2}\left(\frac{\partial \chi_p^{ij}}{\partial y_q} + \frac{\partial \chi_q^{ij}}{\partial y_p} \right)$ and $\varepsilon_{pq}^{0\,(ij)}$ are linearly independent test deformations on the base cell, employed to define the characteristics of the deformations field $\varepsilon_{pq}^{*\,(ij)}$. Here, χ^{ij} are solutions to the following problem

$$\int_Y (\varepsilon_{pq}^{0(ij)} - \varepsilon_{pq}^{*(ij)}) C_{pqrs}\varepsilon_{rs}^{*}(v^{kl})\, d\,Y \quad \forall\ \mathbf{v} \in \mathbf{V}_Y$$

defined on the elementary periodic cell, and $\mathbf{V}_Y = \mathbf{v}(\mathbf{y})$ stands for the set of sufficiently smooth functions obtained in Y and exhibiting Y periodicity.

For 2D problems, there are three test deformation fields that take the following form: $\varepsilon_{pq}^{0\,(11)} = [1\ 0\ 0]$, $\varepsilon_{pq}^{0\,(22)} = [0\ 1\ 0]$ and $\varepsilon_{pq}^{0\,(12)} = [0\ 0\ 0{,}5]$ [41] (symmetry $\varepsilon_{pq}^{0\,(12)} = \varepsilon_{pq}^{0\,(21)}$ implies reduction in the number of test fields from four to three).

Let us consider a 2D elementary periodic cell of a symmetric microstructure (Fig. 1a) made from an isotropic material. In the case of the plane stress-strain state, the governing equations have the following form

$$\begin{bmatrix} \bar{\sigma}_{11} \\ \bar{\sigma}_{22} \\ \bar{\sigma}_{12} \end{bmatrix} = \begin{bmatrix} C^e_{1111} & C^e_{1122} & 0 \\ C^e_{1122} & C^e_{1111} & 0 \\ 0 & 0 & C^e_{1212} \end{bmatrix} \begin{bmatrix} \bar{\varepsilon}_{11} \\ \bar{\varepsilon}_{22} \\ 2\bar{\varepsilon}_{12} \end{bmatrix}. \tag{7}$$

For the isotropic tensor, the homogenized elastic tensor C^e_{ijkl} has three components $C^e_{1111},\ C^e_{1122},\ C^e_{1212}$. If initial deformation ε^0 occurs in the x-direction ($\varepsilon^0_{11} = 1,\ \varepsilon^0_{12} = 0,\ \varepsilon^0_{22} = 0$), then equation (6) yields

$$C^e_{1111} = \frac{1}{|Y|}\int_Y (C_{1111} - C_{1111}\varepsilon_{11}^{*\,(11)} - C_{1122}\varepsilon_{22}^{*\,(11)})\, d\,Y. \tag{8}$$

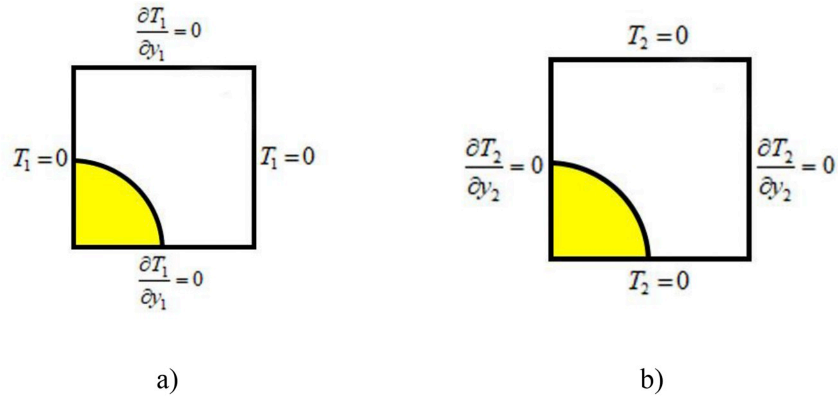

Fig. 2. Boundary conditions for the heat problems (a), (b).

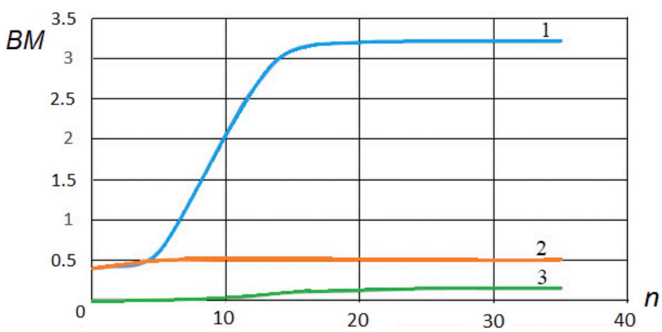

Fig. 3. Convergence of the maximization process of the bulk modulus (number of iterations n are marked on the horizontal axis, whereas numerical values of the bulk modulus (BM) refer to the vertical axis).

Taking into account initial stresses ε^0 in the y-direction ($\varepsilon_{11}^0=0,\ \varepsilon_{12}^0=0,\ \varepsilon_{22}^0=1$), one gets

$$C_{1122}^e=\frac{1}{|Y|}\int_Y (C_{1122}-C_{1111}\varepsilon_{11}^{*(22)}-C_{1122}\varepsilon_{22}^{*(22)})\,d\,Y. \tag{9}$$

If we consider shear initial stresses ε^0 ($\varepsilon_{11}^0=0,\ \varepsilon_{12}^0=0{,}5,\ \varepsilon_{22}^0=0$), then formula (6) yields

$$C_{1212}^e=\frac{1}{|Y|}\int_Y (C_{1212}-2C_{1212}\varepsilon_{12}^{*(12)})\,d\,Y. \tag{10}$$

Now, from (7)–(10) we obtain

$$K^e=(C_{1111}^e+C_{1122}^e)/2,\ \ G^e=C_{1212}^e/2, \tag{11}$$

where K^e/G^e is the effective bulk/shear model.

It is necessary to impose corresponding periodic boundary conditions on the characteristic displacement fields χ. However, in the case when periodic cell exhibits symmetry, the periodicity conditions can be replaced by typical boundary conditions. Namely, if the composite material consists of isotropic components and the periodic cell has symmetry along two axes, then problem (4) is reduced to the problem of a quarter of the cell. In the case of the plane stress-strain state for the quarter part of the elementary cell, the mentioned boundary conditions [42] for the characteristic function can be defined as follows (see Fig. 2): $i=j$ (1 or 2) on $y_1=0,\ y_1=Y_1\ \chi_1^{(ij)}=0$ and on $y_2=0,\ y_2=Y_2\ \chi_2^{(ij)}=0$ (Fig. 1b); in the case of load $ij=12$ (or 21) on $y_1=0,\ y_1=Y_1\ \chi_2^{(12)}=0$ and on $y_2=0,\ y_2=Y_2\ \chi_1^{(12)}=0$ (Fig. 1c).

3. Determination of the effective heat transfer coefficient

To calculate the effective heat transfer coefficient of an elementary periodic cell, the homogenization method is applied, and the associated homogenized terms can be obtained from heat transfer equations. According to references [1,2,27,40], the effective coefficient of heat transfer can be defined in the following way

$$k_{ij}^e=\frac{1}{|Y|}\int_Y \left(k_{ij}(y)-k_{ij}(y)_j\frac{\partial\zeta_i}{\partial y_j}\right)dY=\frac{1}{|Y|}\int_Y k_{ij}(y)\left(I-\frac{\partial\zeta_i}{\partial y_j}\right)dY, \tag{12}$$

with a local coordinate y. In contrast to the mechanical problem (6), where homogenized coefficients C_{ijkl}^e are expressed in terms of initial given deformations $\varepsilon_{pq}^{0\,(ij)}$ in the existing finite element programs, it is impossible to set initial values of temperature gradients. One of the methods proposed by the authors to calculate k_{ij}^e is as follows. Employing notation $I-\frac{\partial\zeta_i}{\partial y_j}=\frac{\partial T_i}{\partial y_j}$ [40] and using the scheme analogous to that used to interpolate the local stiffness tensor, the characteristic function T_i is yielded by the following PDE

$$\frac{\partial}{\partial y_j}\left[k_{ij}(y)\frac{\partial T_i}{\partial y_j}\right]=0. \tag{13}$$

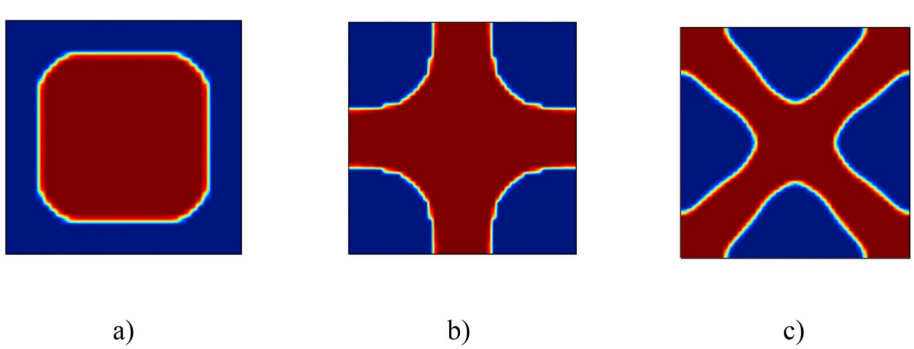

Fig. 4. Optimal microstructures of composites for two competing base materials: (a) maximization $tr(\mathbf{k}^e)$ ($\omega=0$); (b) maximization K^e ($\omega=1$); (c) maximization G^e ($\omega=1$).

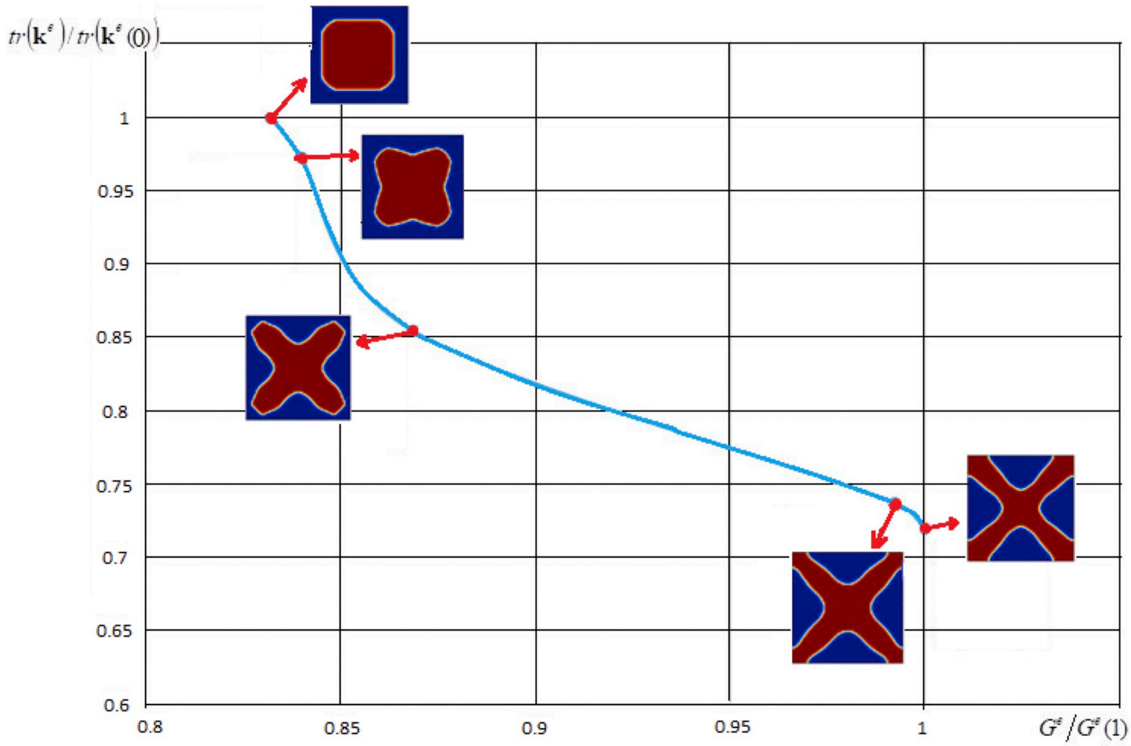

Fig. 5. Optimal topologies from the Pareto set (red/blue colour corresponds to the first/second material). (For interpretation of the references to colour in this figure legend, the reader is referred to the Web version of this article.)

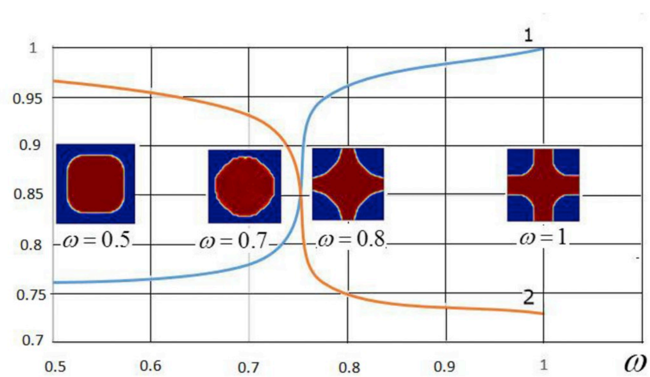

Fig. 6. Relative changes of the effective bulk modulus $K^e(\omega)/K^e(1)$ (1) and heat transfer coefficient $tr(k^e(\omega))/tr(k^e(0))$ (2).

Consequently, the effective heat transfer tensor (12) for an isotropic material with the heat transfer coefficient $k(y_1, y_2)$ can be recast to the following form

$$k_{ij}^e = \frac{1}{|Y|}\int_Y k(y_1, y_2)\frac{\partial T_j}{\partial y_i}dY. \tag{14}$$

For a 2D cell, the effective heat transfer tensor can be presented in the following form

$$\mathbf{k}^e = \begin{bmatrix} k_{11}^e & 0 \\ 0 & k_{22}^e \end{bmatrix}. \tag{15}$$

Therefore, the general effective material conductance can be estimated as follows

$$tr(\mathbf{k}^e) = k_{11}^e + k_{22}^e. \tag{16}$$

Now the boundary conditions [40] for the characteristic functions T_i for a representative cell which take the classical form, are shown in Fig. 2 a,b and have the following form:

for k_{11}^e

$$T_1(0, y_2) = 0, \quad T_1(1, y_2) = 1, \quad \frac{\partial T_1}{\partial y_1}(y_1, 0) = \frac{\partial T_1}{\partial y_1}(y_1, 1) = 0,$$

for k_{22}^e

$$T_2(y_1, 0) = 0, \quad T_2(y_1, 1) = 1, \quad \frac{\partial T_2}{\partial y_2}(0, y_2) = \frac{\partial T_2}{\partial y_2}(1, y_2) = 0.$$

4. Topological optimization

The method of homogenization [1–3] is one of the most effective approaches to compute the global physical properties of a composite, such as the bulk stiffness modulus, the shear modulus or the heat transfer coefficient.

Having both the elastic and thermal homogenization determined, one can define an optimization problem aimed at defining the optimal topology for thermoelastic problems. Such problems are particularly interesting when the elastic and thermal properties of materials strongly compete with each other and the optimal topologies for individual problems differ significantly from each other. To solve the problem, it is necessary to simultaneously take into account both the elastic and thermal material properties.

Let us assume that the elementary periodic cell is divided into finite elements and each finite element has its own variable density ρ_n ($n = 1, ..., N$). Following the rule of SIMP [40], where the role of the control variable is played by an artificially introduced density $\rho_n(\mathbf{x})$, the corresponding Young's modulus $E(\mathbf{x})$ and heat transfer coefficient $k(\mathbf{x})$ for the two-component composite in the n-th finite element can be written as

$$E_n(\mathbf{x}) = E_1\rho_n^p(\mathbf{x}) + E_2(1 - \rho_n^p(\mathbf{x})),$$

$$k_n(\mathbf{x}) = k_1\rho_n^p(\mathbf{x}) + k_2(1 - \rho_n^p(\mathbf{x})),$$

Table 1
Optimal microstructures and values of effective moduli.

ω	0	0.2	0.7	0.775	1
	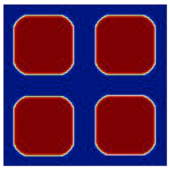	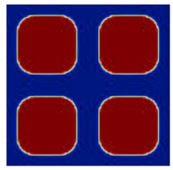	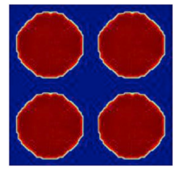	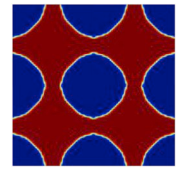	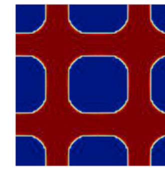
K^e	2.4288	2.4545	2.5100	3.0513	3.2190
$tr(\mathbf{k}^e)$	2.3640	2.3401	2.2027	1.8002	1.7249
ω	0	0.2	0.5	0.715	1
	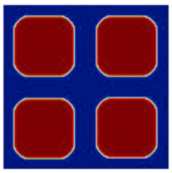	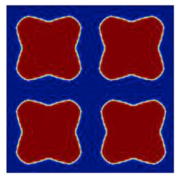	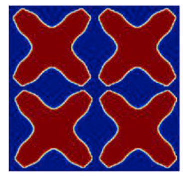	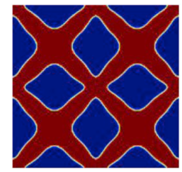	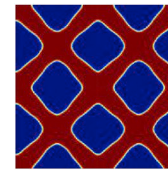
G^e	1.6191	1.6348	1.6900	1.9314	1.9463
$tr(\mathbf{k}^e)$	2.3640	2.2099	1.9413	1.6744	1.6331

Table 2
Optimal microstructures and values of effective moduli for a composite with circular holes.

ω	0	0.2	0.5	1
	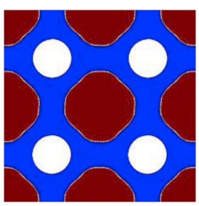	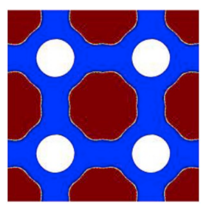	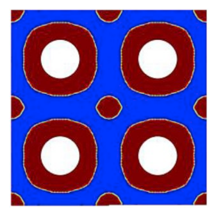	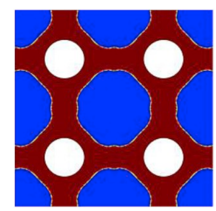
K^e	15281	1.5809	2.1414	2.5262
$tr(\mathbf{k}^e)$	1.9783	1.9382	1.8334	1.3070
	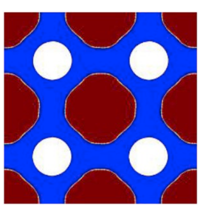	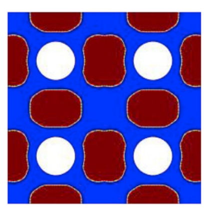	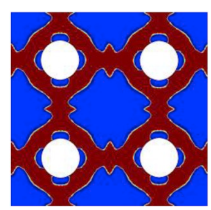	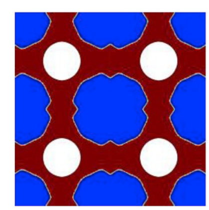
G^e	1.2160	1.3434	1.5361	1.6338
$tr(\mathbf{k}^e)$	1.9783	1.8326	1.3626	1.2438

where E_1, E_2 are Young's moduli of the materials, and k_1, k_2 are the heat transfer coefficients of the materials.

The exponent $p \geq 1$ is used as a penalty factor and the increase in p leads to a clearer decomposition of the material phases (typically $p = 4$ or $p = 5$ [41]).

Usually, for the convenience of calculations, optimization problems with respect to the maximum are reduced to the minimum.

Let M^e denote one of the mechanical quantities, i.e., the effective bulk modulus K^e or the effective shear modulus G^e. The target function is defined as follows

$$\min\left\{(q-1)\left(\frac{\omega\ \mathrm{M}^e}{\mathrm{M}_b} + \frac{(1-\omega)tr(\mathbf{k}^e)}{k_b}\right) + q\frac{h_0 h_{\max}}{A}\int_Y |\nabla\rho(\mathbf{y})|^2 dY\right\}, \tag{18}$$

where: ω – weight coefficient taking into account the input of target functions of the elastic and thermal terms and M_b; k_b – given values of the effective elastic modulus (shear modulus or bulk effective modulus) and the heat transfer coefficient used for the normalization purpose. The second term is the penalty function to exclude the so-called chessboard effect in the optimization process; h_0 is the initial mesh size and $h_{\max}$ is the current mesh size. The quantity $0 \leq q \leq 1$ plays the role of a coefficient that makes it possible to balance the target function and penalty function. It should be noted that the search for the minimum of function (18) corresponds to the search of the function maximum standing next to the multiplier $(q-1)$, since $q-1 \leq 0$ [27].

The isoperimetric constrains for the artificially introduced density $\rho(\mathbf{x})$ are chosen in the following way

$$0 \leq \int_Y \rho(\mathbf{y})dY \leq \gamma A, \tag{19}$$

$$0 < \delta \leq \rho(\mathbf{x}) \leq 1. \tag{20}$$

In formula (19) A stands for the total volume of the material of the optimized space Y in the elementary periodic cell for $\rho(\mathbf{x}) = 1$ and γ denotes the material fraction with parameters E_1, k_1.

To obtain a numerical solution, the stiffness cannot disappear entirely. Thus, in inequality (20), we assume that δ is sufficiently small to avoid the occurrence of singularity of the input stiffness matrix in the optimization process.

Table 3
Optimal microstructures and values of effective moduli for a composite with square holes.

ω	0	0.2	0.5	1
	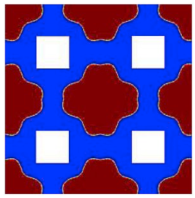	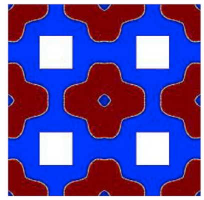	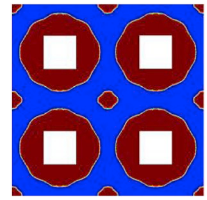	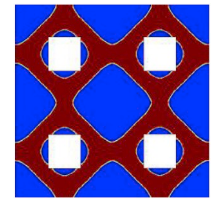
K^e	1.5073	1.5634	2.0590	2.3727
$tr(\mathbf{k}^e)$	1.9035	1.7934	1.8063	1.2943
	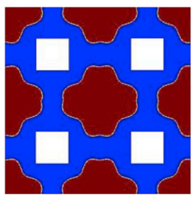	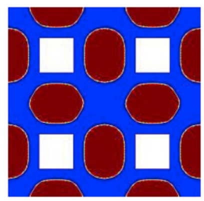	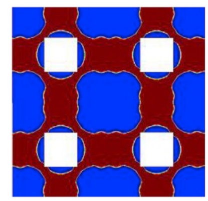	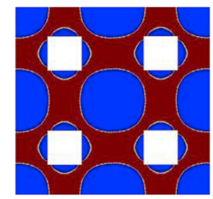
G^e	1.1788	1.2905	1.5709	1.6093
$tr(\mathbf{k}^e)$	1.9035	1.8345	1.2583	1.2422

Table 4
Optimal microstructures and values of effective moduli for a composite with square inclusions.

ω	0	0.2	0.5	1
	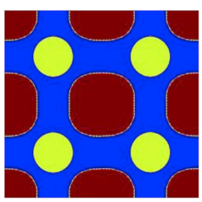	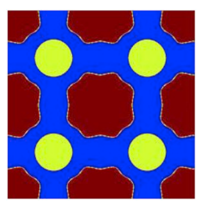	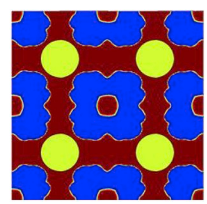	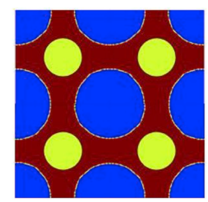
K^e	2.6069	2.6254	3.0512	3.367
$tr(\mathbf{k}^e)$	2.6844	2.6683	1.7779	1.6626
	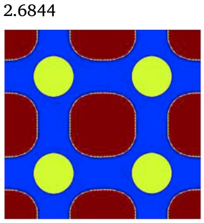	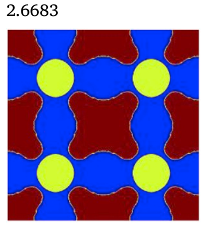	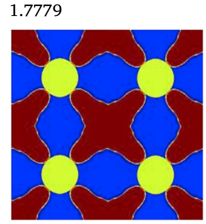	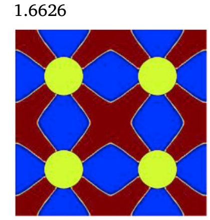
G^e	1.7792	1.8013	1.8782	1.9416
$tr(\mathbf{k}^e)$	2.6844	2.5697	2.3977	1.7052

5. Numerical results

5.1. Topological optimization of a composite made from two competing materials

We consider the elementary cell composed of two competitive materials in the ratio 1:1 ($\gamma = 0{,}5$), i.e., Young's modulus is greater in one material than in the second material, whereas in the second material, the heat transfer coefficient is larger than in the first one. Let us take $E_1 = 1$, $k_1 = 5$ ($E_2 = 5$, $k_2 = 1$) for the first (second) material. The computations were carried out by FEM and the elementary cell was divided into 2500 elements. In order to solve the optimization problem, the method of moving asymptotes (MMA) introduced by Svanberg [12] was employed.

The MMA is based on a special type of convex approximation and it handles element sizes as design variables, shape variables and material orientation angles. In each step of the iterative process, convex approximating subproblems are generated and solved. The latter are controlled by the so called “moving asymptotes” stabilizing and improving the process convergence.

Fig. 3 presents the convergence of the maximization process of the bulk modulus depending on the number of iterations n. Curve 1/2 corresponds to the change in the first/second term of penalty function (18) for $\omega = 1$, whereas curve 3 corresponds to the integral values in inequality (19). At least 25 iterations are required to obtain a sufficiently accurate solution.

First, the problem dealing with the maximization of the effective heat transfer coefficients was solved, i.e. we took the weight coefficient in (18) $\omega = 0$. In all further reported figures, red/blue colour corresponds to the first/second material. Fig. 4a reports the obtained optimal topology for this problem. The optimal value is $tr(\mathbf{k}^e)/2 = 2.364$. The shear modulus and bulk modulus $G^e = 1.619$, $K^e = 2.428$. For the problem dealing with the maximization of the bulk modulus ($\omega = 1$), the optimal topology is presented in Fig. 4b. In this case, the obtained optimal values $K^e = 3.219$, and $tr(\mathbf{k}^e)/2 = 1.725$. For the shear modulus ($\omega = 1$), the optimal topology is shown in Fig. 4c (the optimal values of $G^e = 1.946$ and $tr(\mathbf{k}^e) = 1.633$).

As it follows from Fig. 4, the optimal microstructures for the maximum heat transfer and mechanical moduli strongly differ from each other. Solutions to the multi-criteria problems should be sought only

Table 5
Optimal microstructures and the effective moduli values.

ω	0	0.2	0.5	1
	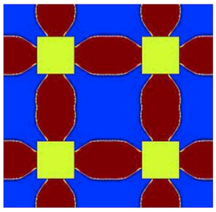	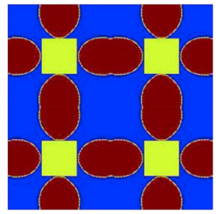	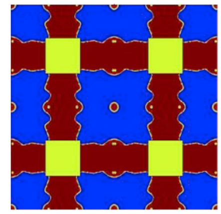	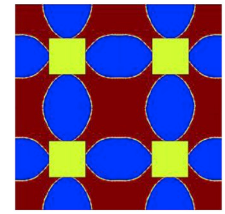
K^e	2.6143	2.7014	3.0023	3.1615
$tr(\mathbf{k}^e)$	2.5402	2.5364	1.8873	1.8085
	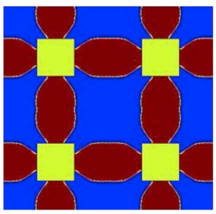	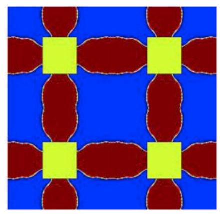	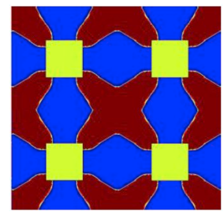	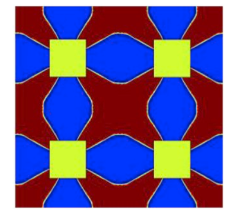
G^e	1.7488	1.7497	1.9005	1.9273
$tr(\mathbf{k}^e)$	2.5402	2.4476	2.4397	1.7220

among the set of alternative optimal solutions in the Pareto sense, i.e., those solutions that could not be substituted by other “better” solutions. Fig. 5 shows optimal topologies depending on the weight coefficient ω for the optimization carried out with respect to two criteria, i.e., the effective shear modulus and the heat transfer coefficient belonging to the set of Pareto solutions [42]. The horizontal axis corresponds to the relative values of the shear modulus $G^e/G^e(1)$, where $G^e(1)$ denotes the optimal value of the shear modulus for $\omega = 1$. The vertical axis presents the relative values of $tr(\mathbf{k}^e)/tr(\mathbf{k}^e(0))$, where $tr(\mathbf{k}^e(0))/2$ stands for the optimal value of the heat transfer coefficient for $\omega = 0$.

When the weight coefficient ω in target function (18) changes, there is a change in priorities of optimization from the criterion of the maximum heat transfer coefficient for $\omega = 0$ up to optimization under the criterion of the maximum bulk modulus or shear modulus.

In Fig. 6, curve 1 shows the relative change in the optimal effective bulk modulus $K^e(\omega)/K^e(1)$, whereas curve 2 presents the analogous value for the heat transfer coefficient.

Fig. 6 shows that in the case study devoted to the optimization of the bulk modulus for $\omega \approx 0.75$, there is a change in priorities in the target function. For $\omega < 0.75$, the priority is given to the maximization of the heat transfer coefficient, whereas for $\omega > 0.75$, the bulk modulus is maximized. The optimal constructions obtained for ω close to the threshold point $\omega = 0.75$ strongly depend on the initial approximation, and the values of their effective moduli exhibit a sudden change when transiting through $\omega = 0.75$.

Table 1 presents the optimal topologies, the values of the effective mechanical moduli, and heat transfer coefficients for different values of ω.

In the considered example, the balance is reached for K^e/G^e for the fixed weight coefficient $\omega \approx 0.75/\omega \approx 0.7$. One can see from Table 1 that a sudden change in the optimal microstructure occurs precisely in the reported points.

5.2. Topological optimization of composites with technological holes

In addition to continuous structures composed of two competing materials, we also studied composite structures composed of two materials with holes of given a priori forms (shapes).

Consider an elementary composite cell having a technological hole of a circular form and a radius of 0.3, or a cell with a square hole of the same area. As in the previous case, the optimized cell area is filled with two competing materials in a 1:1 ratio, with the same parameters. Table 2 shows the obtained microstructures of composites and the values of effective moduli for the composite with circular holes for various values of ω.

The microstructure optimal with respect to K^e has a similar form to the microstructure obtained for the cell without a hole, whereas the form of the optimal microstructure with respect to the value of $tr(\mathbf{k}^e)$ is similar to the composite without the hole but is shifted by 1/4 of the cell. Optimal topologies for the cell with a hole change more smoothly when changing ω than in the homogeneous cell optimization (the change in the target function priorities takes place without a sudden transition).

Table 3 shows the optimal microstructures as well as values of the effective moduli for the cell with a square hole.

As can be seen in Tables 2 and 3, the presence of holes in the cell significantly changes the microstructures that are optimal with respect to G^e. In contrast to the circular holes, square holes more strongly change optimal topologies for all effective moduli. The transition from the microstructures optimal with respect to heat modulus to the microstructures optimal with respect to mechanical moduli occurs more smoothly than in the case of the optimization of a homogeneous cell.

5.3. Topological optimization of composites with technological inclusions

Let us consider structures containing inclusions of a given form, made from a material different than the previous two. The shape and size of inclusions coincide with the characteristics of holes considered in the previous case. In the figures, the area of inclusions is marked in yellow. Both the shape and location of inclusions is a priori specified, Young's modulus of inclusion $E_{inc} = 3$, and the heat transfer coefficient $k_{inc} = 3$. The ratio of the first and the second material to the remaining space part is equal to 1:1.

The obtained computational results for the composites with circular inclusions are presented in Table 4.

The presence of inclusions of a circular shape, in contrast to the holes, does not fundamentally change the form of topologies for the full optimization of either the mechanical or heat moduli. However, it weakens the transition with the change in the priorities in the target function and increases the values of the optimal effective moduli for all considered criteria.

Table 5 reports the computational results for the composites with the inclusions of a square shape.

The presence of inclusions of a square form strongly affects the topology in solving the heat problem or the problem of the maximum bulk stiffness modulus K^e.

6. Concluding remarks

In this work, problems associated with multifunctional requirements with respect to effective characteristics of composites consisting of two components as well as composites with holes or technological inclusions have been studied. In the process of investigation, a strong dependence of the optimal topology of the distribution of materials in the microstructure of composites on the form of the target functions has been detected.

The study of transformations of the optimal topology of the composite microstructure with a change in the weight coefficient from $\omega = 0$ (maximization of the heat transfer) up to $\omega = 1$ (maximization of the mechanical moduli) has been conducted. Moreover, a set of alternatives optimal in the Pareto sense has been constructed.

The considered examples clearly indicate the inability to achieve the best/required properties simultaneously in both cases, which is caused by conflicting criteria in the target function.

Acknowledgement

This work has been supported by Grant RSF No.16-11-10138.

References

[1] Bensoussan A, Lions J, Papanicolaou G. Asymptotic analysis for periodic structures. Amsterdam: North-Holland; 1978.
[2] Sanchez-Palencia E. Non-homogeneous media and vibration theory. Berlin: Springer Verlag; 1980.
[3] Bendsøe M, Kikuchi N. Generating optimal topologies in optimal design using a homogenization method. Comput Meth Appl Mech Eng 1988;71:197–224.
[4] Andrianov IV, Awrejcewicz J, Danishevskyy VV. Asymptotical mechanics of composites. Berlin: Springer; 2018.
[5] Bendsøe M. Optimal shape design as a material distribution problem. Struct Optim 1989;1:193–202.
[6] Xie Y, Steven G. A simple evolutionary procedure for structural optimization. Comput Struct 1993;49:885–96.
[7] Sethian J, Wiegmann A. Structural boundary design via level set and immersed interface methods. J Comput Phys 2000;163(2):489–528.
[8] Wang M, Wang X, Guo D. A level set method for structural topology optimization. Comput Meth Appl Eng 2003;192:227–46.
[9] Belytschko T, Xiao S, Parimi C. Topology optimization with implicit functions and regularization. Int J Numer Meth Eng 2003;57(8):1177–96.
[10] Allaire G, Jouve F, Toader A. Structural optimization using sensitivity analysis and a level-set method. J Comput Phys 2004;194:363–93.
[11] Zhou M, Rozvany G. Dcoc: an optimality criteria method for large systems, part i: theory. Struct Optim 1993;5:12–25.
[12] Svanberg K. The method of moving asymptotes – a new method for structural optimization. Int J Numer Meth Eng 1987;24:359–73.
[13] Sethian J, Wiegmann A. Structural boundary design via level set and immersed interface methods. J Comput Phys 2000;163(2):489–528.
[14] Sigmund O. Materials with prescribed constitutive parameters: an inverse homogenization problem. Int J Solid Struct 1994;31:2313–29.
[15] Sigmund O. Tailoring materials with prescribed elastic properties. Mech Mater 1995;20:351–68.
[16] Sigmund O, Torquato S. Design of materials with extreme thermal expansion using a three-phase topology optimization method. J Mech Phys Solid 1997;45:1037–67.
[17] Larsen U, Sigmund O, Bouwstra S. Design and fabrication of compliant micromechanisms and structures with negative Poisson's ratio. J Microelectromech Sys 1997;6(2):99–106.
[18] Sigmund O. A new class of extremal composites. J Mech Phys Solid 2000;48:397–428.
[19] Gibiansky L, Sigmund O. Multiphase elastic composites with extremal bulk modulus. J Mech Phys Solid 2000;48:461–98.
[20] Li Q, Steven G, Xie Y, Qurein O. Shape and topology design for heat conduction by evolutionary structural optimization. Int J Heat Mass Tran 1999;42:3361–71.
[21] Jonsmann J, Sigmund O, Bouwstra S. Compliant thermal microactuators. Sensor Actuator 1999;76:463–9.
[22] Rodrigues H, Fernandes P. A material based model for topology optimization of thermoelastic structures. Int J Numer Meth Eng 1995;38(12):1951–65.
[23] Li Q, Steven G, Xie Y. Thermoelastic topology optimization for problems with varying temperature fields. J Therm Stresses 2001;24:347–66.
[24] Cho S, Choi J. Efficient topology optimization of thermo-elasticity problems using coupled field adjoint sensitivity analysis method. Finite Elem Anal Des 2005;41(15):1481–95.
[25] Chen X, Mai Y. Micromechanics of rubber-toughened polymers. J Mater Sci 1998;33(14):3529–39.
[26] Hashin Z, Shtrikman S. A variational approach to the theory of the elastic behaviour of multiphase materials. J Mech Phys Solid 1963;11:127–40.
[27] Guest J, Prevost J. Optimizing multifunctional materials: design of microstructures for maximized stiffness and fluid permeability. Int J Solid Struct 2006;43:7028–47.
[28] Prager W, Taylor J. Problems of optimal structural design. J Appl Mech 1968;35:102–6.
[29] Torquato S, Hyun S, Donev A. Optimal design of manufacturable three-dimensional composites with multifunctional characteristics. J Appl Phys 2003;94(9):5748–55.
[30] Yoo J, Lee C. Topology optimization of a swing arm type actuator using the response surface method. Microsys Tech Micro Nanosys Inf Stor Process Sys 2007;13(1):21–31.
[31] Seresta O, Gürdal Z, Adams DB, Watson LT. Optimal design of composite wing structures with blended laminates. Comp Part B 2007;38:469–80.
[32] Bassir DH, Irisarri FX, Maire JF, Carrere N. Incorporating industrial constraints for multiobjective optimization of composite laminates using a GA. Int J Simul Multidiscip Des Optim 2008;2:101–6.
[33] Lee DS, Morillo C, Bugeda G, Oller S, Onate E. Multilayered composite structure design optimisation using distributed/parallel multi-objective evolutionary algorithms. Compos Struct 2012;94(3):1087–96.
[34] Ning F, Cong W, Qiu J, Wei J, Wang S. Additive manufacturing of carbon fiber reinforced thermoplastic composites using fused deposition modelling. Compos Part B 2015;80:369–78.
[35] Madeira JFA, Araujo AL, Mota Soares CM. Multiobjective optimization of constrained layer damping treatments in composite plate structures. Mech Adv Mater Struct 2017;24(5):427–36.
[36] Salem AI, Donaldson SL. Weight and cost multi-objective optimization of hybrid composite sandwich structures. Int J Comput Meth Exp Measur 2017;5(2):200–10.
[37] Seretis G, Kouzilos G, Manolakos D, Provatidis Ch. Multi-objective curing cycle optimization for glass fabric/epoxy composites using Poisson regression and genetic algorithm. Mater Res 2018;21(2):e20170815.
[38] Passos AG, Luersen MA. Multiobjective optimization of laminated composite parts with curvilinear fibers using Kriging-based approaches. J Struc Multidisci Optim 2018;57(3):1115–27.
[39] Awrejcewicz J, Pavlov SP, Bodyagina KS, Zhigalov MV, Krysko VA. Design of composite structures with extremal elastic properties in the presence of technological constraints. Compos Struct 2017;174:19–25.
[40] Bakhvalov NS, Panasenko G. Homogenisation: averaging processes in periodic media. Netherlands: Springer; 1989.
[41] Andrianov IV, Awrejcewicz J, Danishevs'kyy VV, Ivankov AO. Asymptotic methods in the theory of plates with mixed boundary conditions. Wiley; 2014.
[42] Pareto V. Manual of political economy. New York: Macmillan; 1971.
[43] Alizadeh AN, Sofiyev AH. Modified Young's moduli of nano-materials taking into account the scale effects and vacancies. Meccanica 2011;46:915–20.